Rafik Halimi^{a,b}, Boudjema Bezzazi^b, Ali Badidi Bouda^a, M'hamed Djelloul Abbou^c, Oussama Mimouni^c

- ^a Welding and NDT Research Center (CSC), Cheraga, Algeria
- ^bResearch Unit Materials, Processes and Environment, University of Boumerdes, Boumerdes, Algeria
- ^cResearch and Development Center of Aeronautical Mechanics, Dar-El Beida, Algeria

Study and analysis of mechanical and viscoelastic behavior in flexure of laminated composites

In the present paper, seven laminated composites were the subject of an experimental study to determine their mechanical and viscoelastic properties by means of dynamic mechanical analysis in a bending configuration. The influence of the frequency, fiber type and fiber orientation on dynamic mechanical properties of different system composites were investigated. Carbon/epoxy laminates exhibit a great stiffness when fibers are oriented along the axis of the clamps, and the maximum modulus was reported for unidirectional carbon/epoxy laminate [08 plies] with 56.4 GPa. The glass transition temperature was found to decrease with the incorporation of fibers and increase with increased frequency. For the Kevlar/epoxy laminate, an increase of 12.5 °C in glass transition temperature was observed. This is related to a better interfacial adhesion between epoxy matrix and Kevlar fibers.

Keywords: Composite laminate; Dynamic mechanical analysis; Fiber/matrice interface; Glass transition temperature

1. Introduction

The use of thermosetting composite materials has enjoyed a significant growth in many industrial applications due to high mechanical properties and low density [1, 2]. Nevertheless, the mechanical performance of a composite materials depends not only on the properties of the reinforcement (type, orientation, geometry) and on those of the matrix, but also on the quality (cohesion, durability) of the interfacial zone which guarantees reinforcement/matrix compatibility. This latter is ensured by a distribution of the stress loads between the two components. As a consequence, the degradation of the interfacial zone results in structural damage such as fibers-matrix decohesion or delamination which will impact the properties of the final composite [3-5]. During their in-service use, composite materials are subjected to mechanical stresses or exposed to different environmental conditions involving temperature and humidity [6, 7]. At high temperatures above their glass transition temperature (T_{o}) , a thermosetting polymer undergoes three transitions in its structural state, marked by two temperatures: the T_g observed during the amorphous phase of the polymer and the decomposition temperature (T_d) at which covalent bonds of the macromolecular skeleton start to

break under the action of thermal energy transferred to molecules [8].

According to Bai et al. [9], when temperature exceeds the $T_{\rm g}$, the polymeric material shifts from a glassy state to a rubbery one due to the breaking of the covalent bonds of the molecules (activation energy). This transition is followed by a degradation of the physicochemical properties of the matrix (break of the weak chemical bond and more specifically of its interface with fibers). It is at this interface level that thermal stress concentration starts, owing to the difference in the expansion coefficients between fibers and matrix. Such a phenomenon translates into the appearance of micro deteriorations (interlaminar cracks) and into the decohesion of the fiber/matrix interface [10–12].

Currently, the dynamic mechanical analysis (DMA) technique is widely used for the experimental study of polymeric matrix composites [13-15]. It is based on the material's response to sinusoidal mechanical stresses as a function of temperature, frequency and time; enabling the measurement of relaxation phenomena in polymers [16]. DMA allows the determination of the different transitions polymeric materials undergo as a function of temperature, and hence, making it possible to evaluate the viscoelastic properties of materials by means of their elasticity modulus (storage modulus E'), loss modulus E'', and loss factor (damping factor $\tan \delta$) [17]. Therefore, a lot of information can thus be gained. Beside the determination of mechanical transition temperatures [18], we can, through isochronous or isothermal tests, study molecular relaxation phenomena within the material (activation energy, time, relaxation characteristics) [19]. Along this line, some studies used DMA to evaluate fiber/matrix interfacial adherence.

Thomason [20] used DMA to characterize the interfacial zone of composites by measuring the glass transition temperature of the matrix and observing its development as a function of the nature of the interface. Indeed, an increase in the glass transition may indicate a stiffening of the interfacial zone due to better fiber/matrix interaction. Khatibi and Mai [21] demonstrated that a relation exists between $\tan \delta$ peak and the interfacial adhesion strength, which can give a real indication about molecular motion. The higher is the molecular motion, the larger is the area under the $\tan \delta$ peak, and the weaker is the interfacial adherence observed. In fact, all studies have reported the existence of a strong dependence of viscoelastic properties and an increase in $T_{\rm g}$ besides other parameters like frequency, heat-

Table 1. Designation and properties of different fibers.

Reinforcement type	Style	Weight (g m ⁻²)	Density (g cm ⁻³)	Thickness (mm)	Tensile strength (MPa)	Strain (%)
UD Carbon Woven Carbon Woven E-glass Woven Kevlar	Unidirectional Plain Plain 2 × 2 Twill	230 ± 10 200 ± 10 225 ± 25 197 ± 20	1.76 1.80 2.54 1.45	0.30 0.28 0.25 0.20	4300 3450 3100 2955	1.8 1.5 4.4 2.5

ing rate [14, 22], fiber volume fraction [23], fatigue loading [24] as well as the type and the orientation of fibers [25]. Goertzen and Kessler [14], Karbhari and Wang [22], reported that the $T_{\rm g}$ of carbon/epoxy composite was strongly influenced by heating rate and frequency. Goertzen and Kessler [14] observed that the variation in T_g is more significant with frequency than with heating rate. An increase in the frequency leads to a displacement of the maximum peak of tan δ , which represents $T_{\rm g}$ towards high temperatures. Thomason [20], Melo and Radford [25] investigated the influence of the type of fibers and their orientations on the mechanical and viscoelastic behavior of compsites. The results obtained by Thomason [20] showed that the storage modulus and the loss modulus peaks are higher for carbon fiber than for glass fiber composites. Moreover, the maximum peak of the loss modulus of the different composites is shifted towards higher temperatures, compared to the matrix. By using unidirectional glass fibers, he has also shown that the peak of the loss modulus is shifted to higher temperatures with respect to the untreated matrix. These results are due, according to the author, to the interaction of the interface between fibers and matrix. The subject of our work is therefore to evaluate the mechanical and dynamic properties in flexure of composite laminates. The study investigates the influence of temperature, frequency, the type of fibers and their orientations on the mechanical and viscoelastic behavior of laminates during the loading. It also highlights the interaction of the interface between fibers and matrix.

2. Experimental procedure

2.1. Materials

The composite laminates studied in this work were manufactured using four types of reinforcement: the unidirectional carbon weave fabrics (SikaWrap 230 g m⁻² weight), used in civil engineering for external strengthening of concrete structures, the plain weave carbon [0/90] fabrics (HR 3 K 200 g m⁻² weight) with high mechanical stresses advisable for aircraft construction, the E-glass plain weave [0/90] fabrics (GWR 225 g m⁻² weight) used especially for boat building and the aramid (Kevlar) 2/2 twill weave [0/90] fabrics (KF 197 g m⁻² weight) used for various aeronautical and military applications. The characteristics of the different reinforcement are shown in Table 1.

The matrix used for the preparation of laminates is an epoxy resin, marketed in Algeria by GRANITEX[®], and delivered as pre-dose kit. The matrix consists of a mixture of component A: three-dimensional polymer type: diglycidyl ether of bisphenol (DGEBA), with the element B: aliphatic

amine hardener, carrying the commercial name Medapoxy Primary. The mass ratio between these two components is 0.67. The physical and mechanical characteristics of the matrix are listed in Table 2.

2.2. Preparation of laminates

The laminated composite plates were prepared by vacuum molding, using the 'bagging' technique [26]. This technique consists of gradually replacing the vacuum by a resin, using a vacuum pump, until impregnation of all fibers, and then the vitrification of the resin. Once prepared, they were put in an autoclave at 80 °C for 8 hours to allow polymerization. All laminates had eight plies, with an average thickness of 2 mm. Laminates with unidirectional fibers are referred to as (UDL), the woven carbon fibers as (CL), the woven glass fiber as (GL), while those including woven Kevlar are designated by (KL). The properties of the different composites are given in Table 3.

Table 2. Properties of the epoxy matrix.

Properties	Ероху
Viscosity fit 25 °C (mPa s)	11 000
Density p (g cm ⁻³)	1.18
Young's modulus E (GPa)	2.53
Tensile strength (MPa)	60–70
Flexural strength (MPa)	105
Maximum elongation (%)	3.6
Glass transition temperature $T_{\rm g}$ (°C)	90

Table 3. Description of different composite samples.

Compo- sites	Structure	Density (g cm ⁻³)	Volume fiber fraction (%)	Thickness (mm)
UDL1	[0]8	1.43	49	2.1-2.2
UDL2	$[(0/90)_2]_S$	1.49	47	2.1-2.2
UDL3	[±45] ₈	1.47	50	2.0-2.1
UDL4	[90] ₈	1.41	46	2.0-2.1
CL	[C] ₈	1.45	45	1.9-2.0
GL	[G] ₈	1.87	60	2.0-2.1
KL	[K] ₈	1.35	57	1.6–1.7

2.3. Static bending tests

Static three-point bending tests were performed on $90 \times 11 \times 2 \text{ mm}^3$ specimens, according to ASTM D790 standards [27], which specify the dimensions of test pieces, the distance between the clamps, and the test speed. The tests were conducted on a ZWICK testing machine 2 kN (ZWICK/ROELL, Germany). The monitoring and the data acquisitions were PC-based using testXpert 9.11 software. According to ASTM D790, the flexural strength failure (σ_f), the flexural Strain (ε_f), the flexural modulus (E_f) and the shear strength (τ) were calculated according to the following formulas:

$$\sigma_{\rm f} = \frac{3P_{\rm max}L}{2bh^2} \tag{1}$$

$$E_{\rm f} = \frac{mL^3}{4bh^3} \tag{2}$$

$$\tau_{\text{max}} = \frac{3P_{\text{max}}}{4bh} \tag{3}$$

where P_{max} is the applied force (N), L is the span (mm), b is the width and h is the thickness of the specimen.

2.4. Dynamic mechanical analysis

DMA is used to determine the evolution of the viscoelastic properties as a function of temperature, frequency or time, by applying cyclic deformation [16]. The viscoelastic behavior is generally described as a complex modulus $E^* =$ E' + iE'', where the real part E', called storage modulus, reflects the conservative elastic behavior of the material and an imaginary part E'' (loss modulus) characterizes the viscous and dissipative behavior. The ratio $E''/E' = \tan \delta$ is the tangent of the phase angle, δ , called loss factor. The dynamic mechanical tests were conducted in a three-point bending mode, according to ASTM D4065 [28] and ASTM D5023 [29] standards, using rectangular samples ($50 \times 10 \times$ 12 mm³). The DMA tests were carried out on a NETZSCH dynamical mechanical analyzer DMA 242C (NETZSCH, Germany). The analysis was made over the temperature range (20–200 K) with a heating rate of 3 K min⁻¹ while applying different frequencies: 1, 2, 5, 10 and 20 Hz in static air atmosphere. The deformation amplitude was 0.02 mm, which represents 1% of the height of the sample.

3. Results

3.1. Static bending tests results

The stress-strain curves of the static bending test for the different laminated composites are shown in Fig. 1. Table 4 gives the test results and shows the calculated values of the flexural strength, the flexural strain, the shear strength and the flexural modulus.

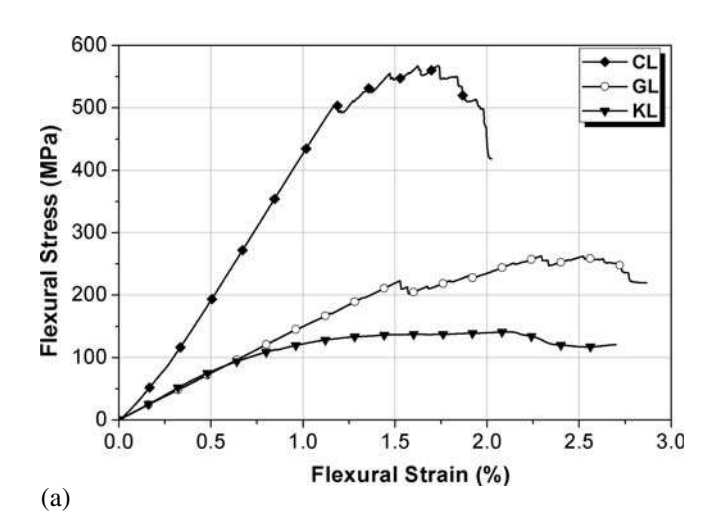
3.2. Failure surfaces examination

Optical and scanning electronic microscopes (SEM) were used to examine the fracture surface of failed specimens after static bending tests; the obtained micrographs are shown in Figs. 2 and 3.

3.3. Dynamic mechanical analysis

3.3.1. Influence of temperature

Figure 4 shows the evolution of the storage modulus E' and the loss factor $\tan \delta$ as a function of temperature for the epoxy resin alone and for UDL1 laminate, at 1 Hz.



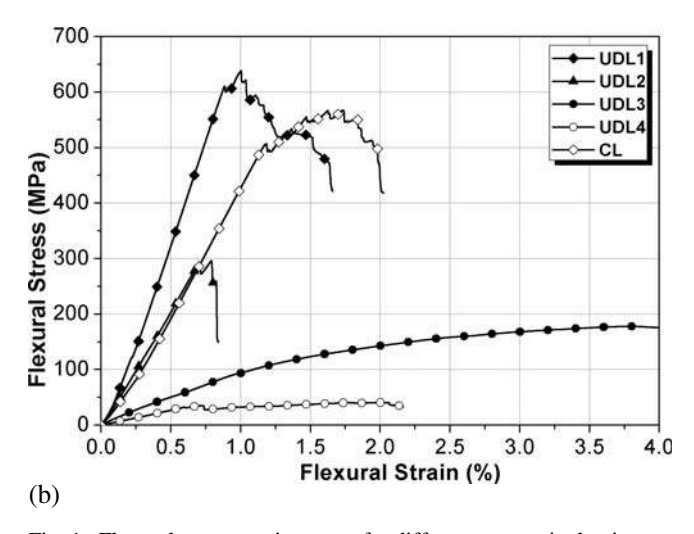


Fig. 1. Flexural stress–strain curves for different composite laminates: (a) fiber type effect, (b) fiber configuration effect.

Table 4. Flexural properties for various composites laminates.

Laminates	Flexural strength (MPa)	Flextural strain (%)	Flexural modulus (GPa)	Shear strength (MPa)
UDL1	639.4	1.00	54.5	7.11
UDL2	296.4	0.79	41.4	3.28
UDL3	177.7	3.75	10.7	1.97
UDL4	34.7	0.72	4.4	0.40
CL	505.2	1.21	29.1	6.31
GL	262.6	1.52	16.0	2.92
KL	141.4	2.10	15.2	1.56

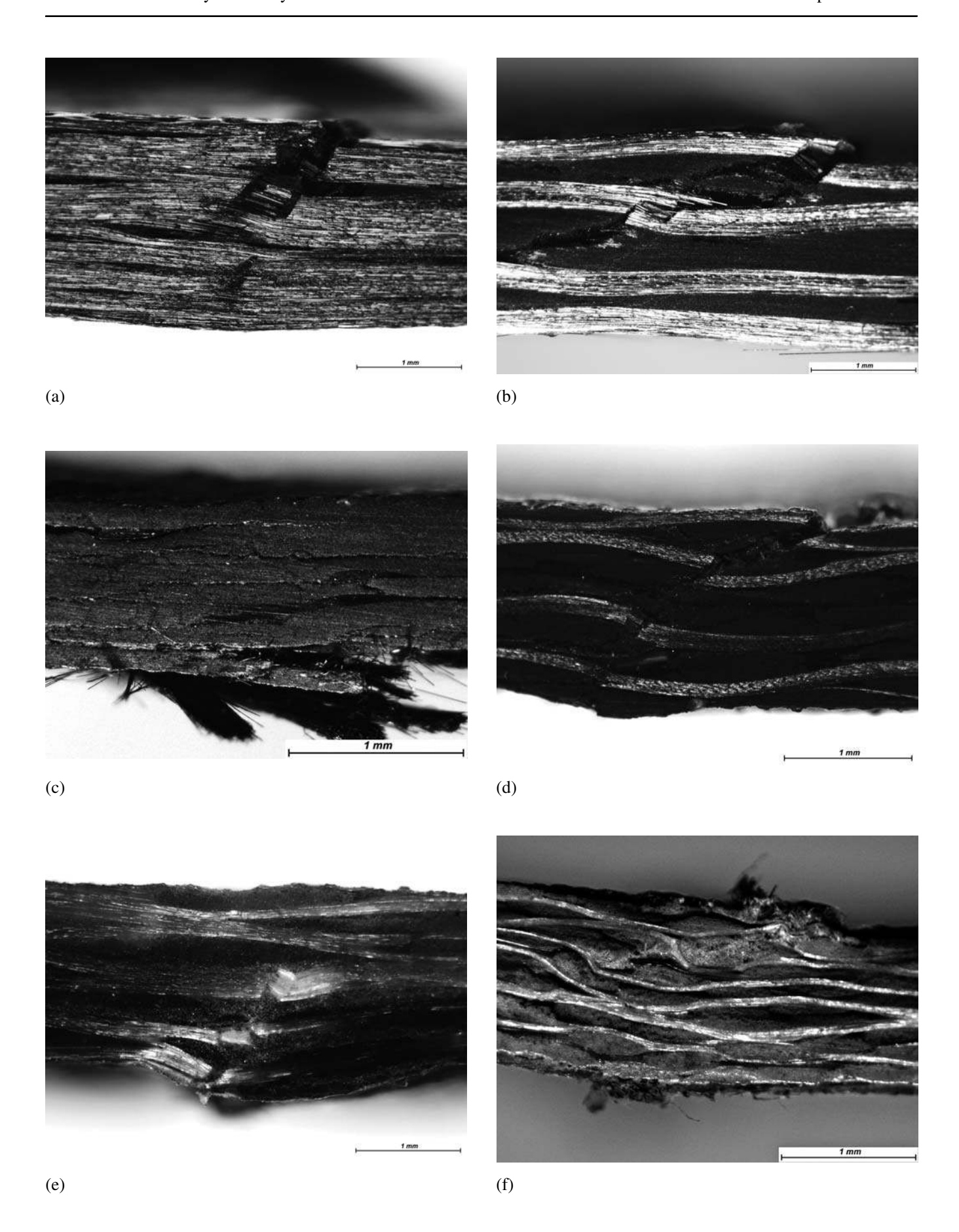


Fig. 2. Optical macrographs of failed laminates: (a) transverse crack and failure of the compressed zone in UDL1, (b) transverse crack, delamination and failure of the compressed zone in UDL2, (c) delamination and failure of the tensile zone in UDL3, (d) transverse crack in CL, (e) transverse crack and failure of the tensile zone in GL and (f) delamination in KL.

3.3.2. Influence of frequency

Figure 5 shows the effect of varying frequency on storage modulus and loss factor with temperature for UDL1 composite laminate. The results of $T_{\rm g}$ measurements for the different composite laminates are gathered in Table 5.

3.3.3. Influence of fiber type

Figure 6 shows the variation of storage modulus and damping factor as a function of temperature for CL, GL, KL

composite laminates at 1 Hz. Table 6 contains the results of the DMA test for the matrix and various laminates.

3.3.4. Influence of fiber configuration

Figure 7 shows the variation of the storage modulus and loss factor as a function of temperature at 1 Hz, for the five configurations of carbon/epoxy composites. Table 7 shows a summary of DMA tests for alone matrix and different configurations of composites.

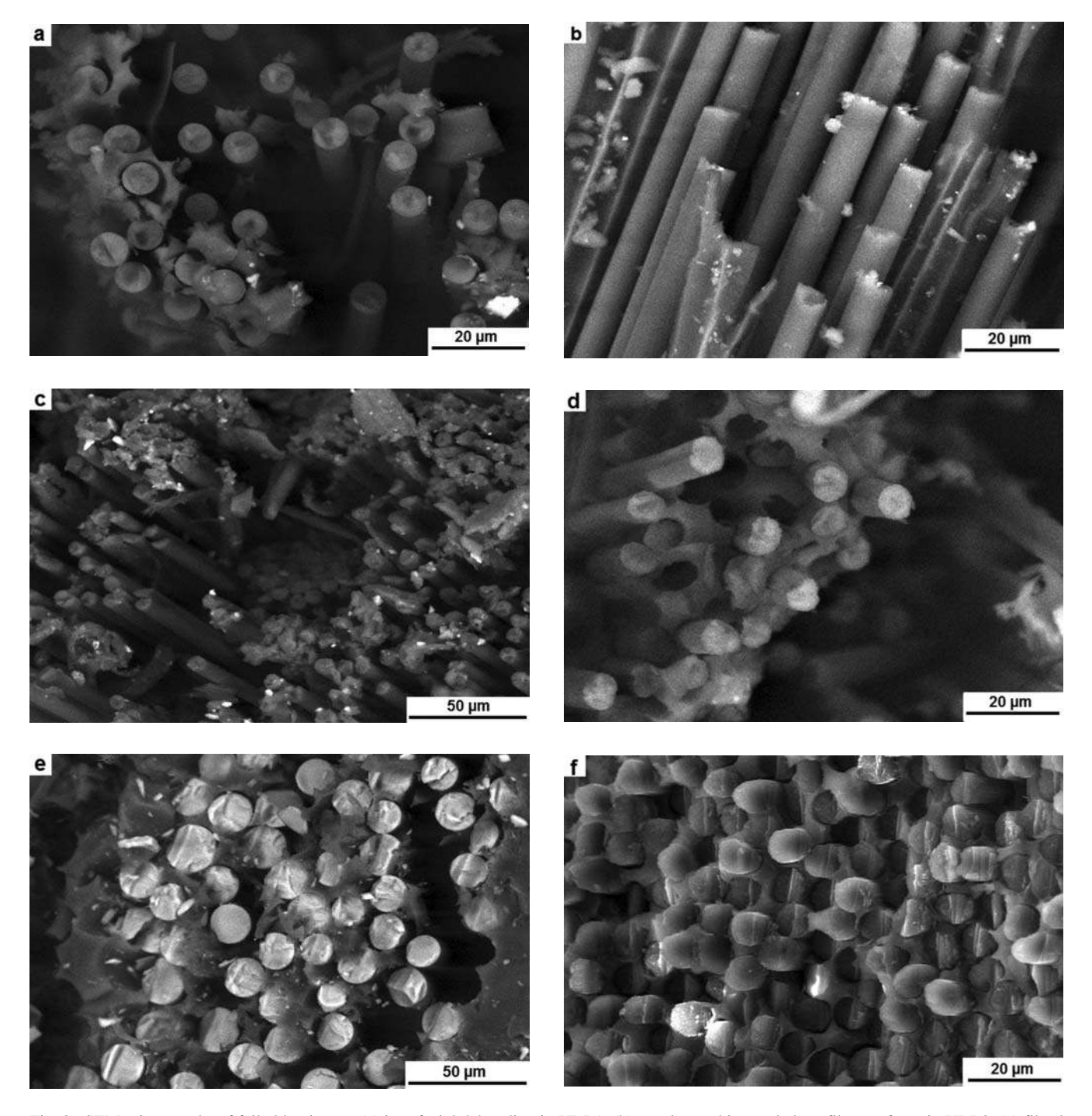


Fig. 3. SEM micrographs of failed laminates: (a) interfacial debonding in UDL1, (b) matrix cracking and clean fiber surfaces in UDL2, (c) fiber/matrix splitting in UDL3, (d) fiber pullout in CL, (e) matrix cracking and fiber/matrix debonding in GL and (f) fiber breakage and little fiber slippage indicate good fiber/matrix adhesion in KL.

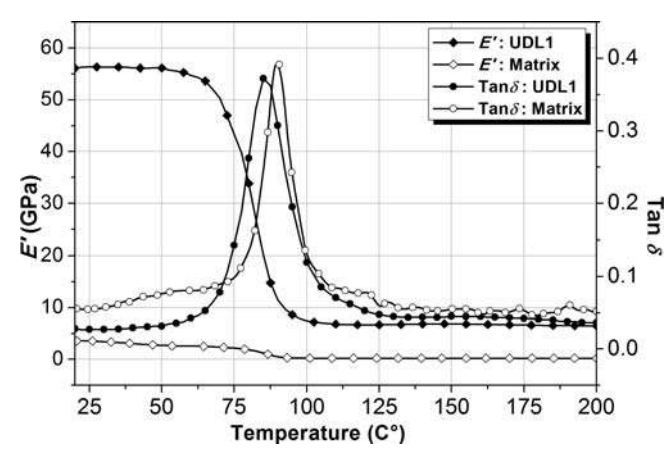


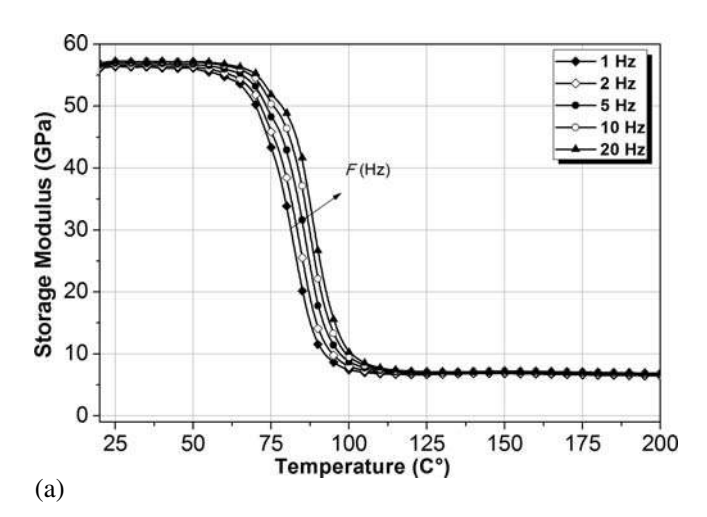
Fig. 4. Variation of storage modulus and damping factor as a function of temperature for the matrix and UDL1 composite laminate at 1 Hz.

4. Discussion

4.1. Bending tests results

According to the results shown in Fig. 1a, the CL composite is the stiffest at about 29.1 GPa and displays the least strain value of 1.21 %, then comes the GL composite with flexural modulus value of 16 GPa and strain up to 1.52 %. Finally, KL composite that presents a flexural modulus value of 15.2 GPa and strain of 2.1 %.

It can be seen from Fig. 1b, that the stiffest laminate possesses a maximum of plies oriented at 0° relative to the axis of the laminate. An increase in the thickness of 0° oriented plies results in an increase of both the stiffness and the flexural strength [30]. The results show that UDL1 laminate, which has a maximum of plies (08 plies) oriented at 0° relative to the axis of the laminate, is the stiffest about 54.5 GPa and exhibits the highest stress value of 639.4 MPa. Followed by UDL2 laminate (04 plies) with flexural modulus value of 41.4 GPa and stress of 296.4 MPa, then comes UDL3 and UDL4 with flexural modulus values of 10.7 GPa and 4.4 GPa, corresponding to stress values of 177.7 MPa and 34.7 MPa respectively. Regarding UDL3 and KL laminates, we notice that the maximum flexural strengths are lower, and large strains (deformations) are observed at maximum stress failure. This is due to a slippage of the interfaces between plies (delamination), which are less loaded with shear stresses.



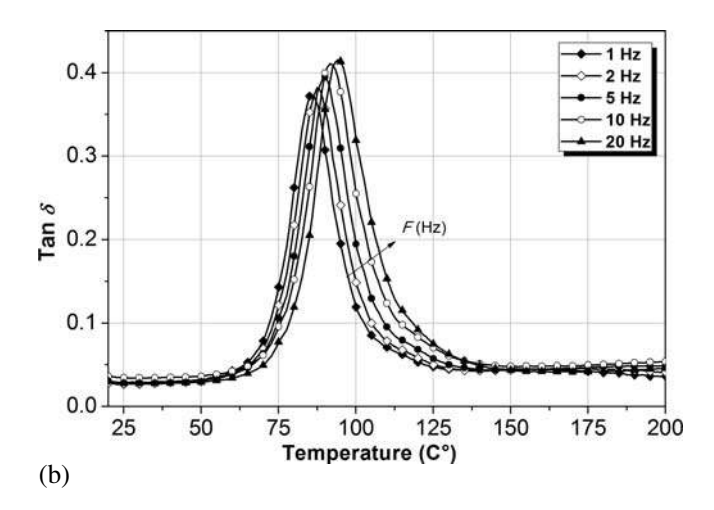


Fig. 5. Dynamic data of UDL1 laminate for different frequencies: (a) Storage modulus vs. temperature, (b) $\tan \delta$ vs. temperature.

Figures 2 and 3 show three types of damage in three fracture zones: tensile at the lower zone, shear at the intermediate, and compression at the upper one, which is the most predominant one. Bezazi et al. [30] have previously observed these damages on glass/epoxy and Kevlar/epoxy laminates during flexural tests. Zhang et al. [31] reported the same regarding carbon/epoxy, glass/epoxy composites and their different hybridizations.

Table 5. Measured T_g as a function of frequency for various composites, obtained from E' and tan δ curves.

Frequen- cy (Hz)	$T_{\rm g}(^{\circ}{ m C})$													
Cy (IIZ)	UDC1 UDC2		UDC3		UE	UDL4		CL		KL		GL		
	E'	$ an \delta$	E'	$ an \delta$	E'	$ an \delta$	E'	$ an\delta$	E'	$ an \delta$	E'	$ an\delta$	E'	$ an\delta$
1	67.8	85.7	72.3	83.6	52.5	82.0	71.6	85.7	74.6	86.1	83.6	102.5	72.0	82.5
2	71.2	87.5	74.6	85.4	54.2	84.6	73.3	86.8	76.2	88.3	85.2	105.7	75.4	84.4
5	74.1	89.6	77.0	87.8	56.3	87.1	76.0	88.7	78.5	90.5	87.5	110.4	78.1	86.5
10	77.1	91.7	79.6	89.9	58.4	88.9	78.6	90.8	80.8	92.6	89.4	114.0	79.2	88.6
20	80.2	94.1	81.0	92.5	60.5	91.1	80.1	93.1	83.1	95.5	92.1	120.1	80.4	91.5

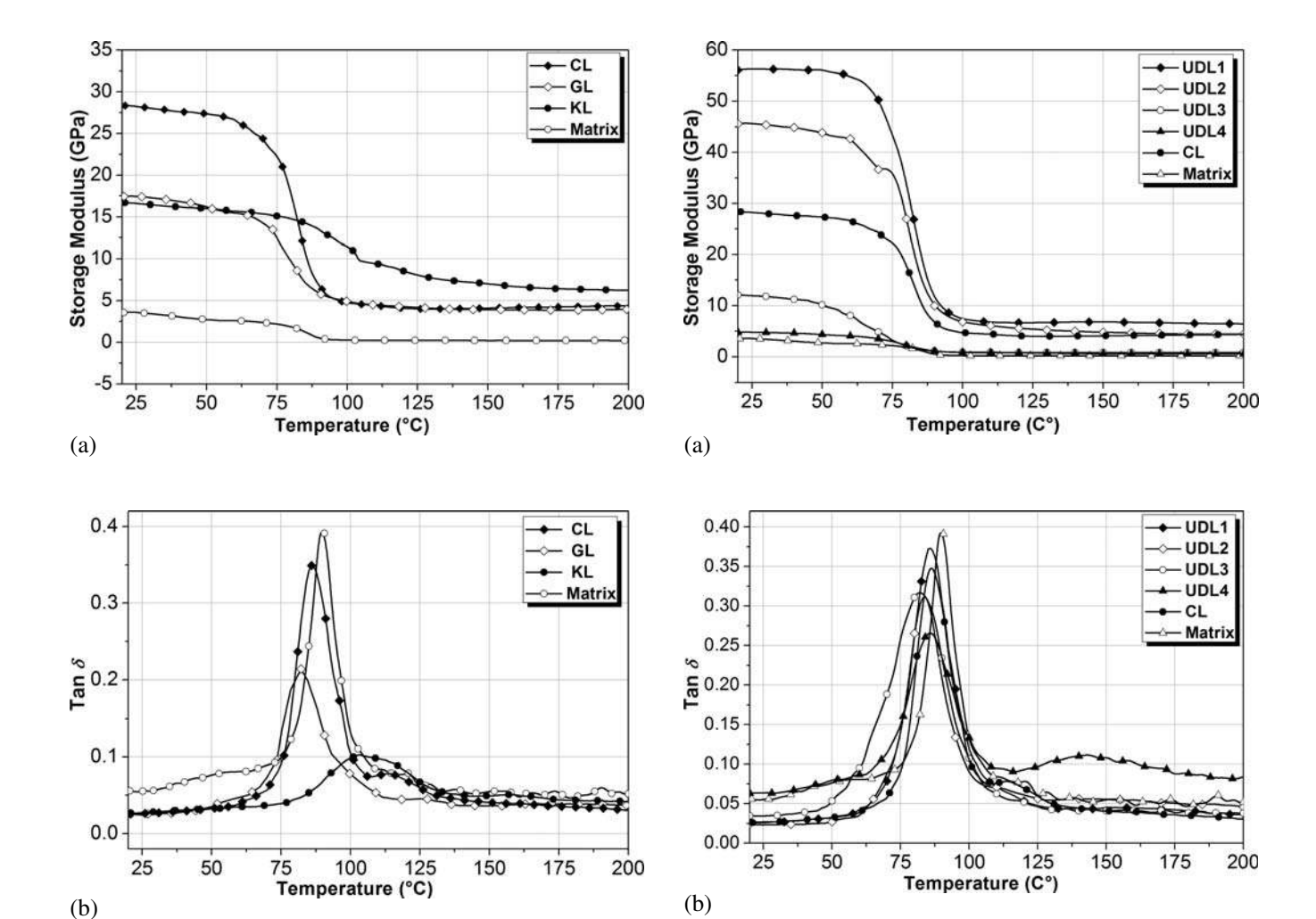


Fig. 6. Effect of fiber type on dynamic data at 1 Hz: (a) storage modulus vs. temperature, (b) $\tan\delta$ vs. temperature.

Fig. 7. Effect of fiber configuration on dynamic data at 1 Hz: (a) storage modulus vs. temperature, (b) $\tan\delta$ vs. temperature.

Table 6. DMA data for different types of composite laminates at 1 Hz.

Laminates	E' at 25 °C (GPa)	E' at 150°C (GPa)	Loss of <i>E'</i> (%)	Tan δ Max peak	$T_{ m g}$ from Tan δ (°C)	$T_{\rm g}$ from E' max (°C)
CL	28.8	4.0	86	0.34	86.1	74.6
GL	17.3	4.0	76	0.21	82.5	72.0
KL	16.4	7.1	56	0.10	102.5	83.6
Matrix	3.6	0.2	94	0.39	90.0	81.1

Table 7. DMA data for different configuration of composite laminates at 1 Hz.

Laminates	E' at 25 °C (GPa)	E' at 150 °C (GPa)	Loss of E' (%)	Tan δ Max peak	$T_{ m g}$ from Tan δ (°C)	$T_{\rm g}$ from E' max (°C)
UDL1	56.4	6.7	88	0.36	85.7	67.8
UDL2	45.7	5.0	89	0.30	83.6	72.3
UDL3	12.2	0.6	95	0.31	82.0	52.5
UDL4	4.8	0.6	87	0.26	85.7	71.6
CL	28.8	4.0	86	0.34	86.1	74.6
Matrix	3.6	0.2	94	0.39	90.0	81.1

In comparison of UDL1, UDL2 and CL laminates, the failure occurs firstly in the upper surface, which is strained by the transverse cracks initiated at 90°, then in the middle by interlaminar segregation (delamination between plies) until complete fracture of the laminate. This is due to the interfaces between fibers and matrix, which are heavily subject to shear stresses. In the case of GL laminate, it can be seen that the samples failed first with a transverse mode by transverse cracks in the 90° fibers, causing delamination between 0° and 90° layers and then to the failure of the fibers of the lower surface in tensile. The UDL3 and KL laminates show very little damage by transverse cracking and the main failure is due to delamination between layers.

4.2. Dynamic mechanical analysis

4.2.1. Influence of temperature

The results indicate that the viscoelastic properties of the matrix and the laminates are highly affected by the temperature (Fig. 4). In the case of the matrix, two transitions are observed: a first one at $60\,^{\circ}\text{C}$ and a second one at $90\,^{\circ}\text{C}$. The first transition indicating a β relaxation corresponds to lateral motion of macromolecular strings and localized bond groups, which find sufficient free space to move [16]. By incorporating the fibers to the epoxy matrix as in the case of UDL1 laminate, we observe a noticeable improvement in the storage modulus (stiffness) and a disappearance of the β transition. This latter is attributed to a restriction on the motion of polymer strings, resulting from the presence of fiber/matrix interface.

According to ASTM E1640 [32], the second transition corresponds to T_g which translates into a sharp drop of the storage modulus with a maximum amplitude of $\tan \delta$ peak. Such a result reflects the shift from a glassy state to a rubbery one, which correspond to a collective motion of molecule strings. Below 60 °C, a slow decrease of 3.3 % of the storage modulus and a slight increase of the loss factor, with respect to the initial state, are observed. This is followed by a substantial drop of 27.7% of the storage modulus in the case of the matrix. At temperatures less than or equal the $T_{\rm g}$, a sharp drop about 60% of the storage modulus and an increase in the loss factor, until it reaches the maximum, is reported for both the laminate and the matrix. Above the $T_{\rm e}$, a drop in loss factor and a decrease of 20 % of storage modulus is first reported, then the two parameters stabilize at 125 °C for the two cases.

4.2.2. Influence of frequency

It can be seen that the storage modulus and the loss factor are affected by frequency. An increase in the frequency leads to an increase of the storage modulus over the temperature range $(60-150\,^{\circ}\text{C})$ (the glass transition region). Beyond that range, E' values remain nearly unchanged (Fig. 5a). Figure 5b also shows an increase and a shift in $\tan\delta$ peak amplitude, which corresponds to α relaxation (T_g) towards high temperatures (rubbery domain). This is in agreement with previous experimental studies [14, 22]. According to Karbharin and Wang [22], the variation of T_g with frequency is mainly related to the variation of the activation energy of the glass transition relaxation (mobility of molecular string segments through adherence). The higher

is the frequency (shorter periods), the smaller is the possibility to observe molecular relaxation phenomena. The increment of $\tan \delta$ peak with the increasing of frequency is also associated with the activation energy of the glass transition relaxation. The material indicates a more brittle response reflecting that a large part of mechanical energy, supplied by the oscillating force, was dissipated in the materials as heat (friction and internal motion).

For a 3 K min⁻¹ heating rate, the highest $T_{\rm g}$ variation is found to be for KL laminate 17.6 °C (120.1–102.5 °C), whereas the lowest is found to be for UDL4 laminate 7.4 °C (93.1–85.7 °C). This can be explained by the important activation energy in KL laminate originating from a good interfacial adherence between fibers and matrix. Furthermore, the glass transition variation for CL laminate at a similar heating rate is 9.4 °C (95.5–86.1 °C), a result very close to that found by Goertzen and Kessler [14], which is 9.6 °C.

4.2.3. Influence of fiber type

The results show that at room temperature (25 °C), the storage modulus values are higher compared to those obtained for the matrix alone (Fig. 6a). This can be explained by an attenuation of the macromolecular string motion. This improvement is related to the creation of a fiber/matrix interface during the crosslinking process, which increases the stiffness in the temperature range above the $T_{\rm g}$. From Table 6, it can be seen that the CL composite is the stiffest and exhibits the highest storage modulus of 28.8 GPa at room temperature, whereas the GL and KL laminates are less stiff and exhibit almost similar storage moduli of 17.3 GPa and 16.4 GPa respectively. In the temperature range above the $T_{\rm g}$ (150 °C), the KL composite loses about 56% of its initial storage modulus which correspond to 7.1 GPa, whereas CL and GL composites have an equal storage modulus about 4 GPa with a loss of 86 % and 76 % respectively. The results also reveal a decrease in the tan δ peak amplitude (Fig. 6b), and a slight shift of the T_g towards low temperatures when we move from a matrix alone (90 °C) to CL (86.1 °C) and GL (82.5 °C), this is equivalent to a decrease of 3.9 °C for CL and 7.5 °C for GL. This can be explained by a low energy dissipation resulting from to the incorporation of fibers, which are purely elastic materials. Such results contrast with those found by Thomason [20], who demonstrated that for the different composites, the temperature T_g shifts to higher values with respect to the matrix. On the other hand, an increase in $T_{\rm g}$ value to 102.5 °C for KL composite was observed; this amounts to a shift of 12.5 °C. It is to be pointed out that the properties of fibers in a bending configuration are very poor, those discrepancies in the mechanical properties and viscoelastic behavior can be attributed to the type of the fibers and the quality of fiber/matrix interfaces which develop during the curing of the matrix. Unlike carbon and glass, which are mineral fibers, Kevlar fibers and epoxy matrix share the same organic nature, which leads to a better interaction of the interfaces. The composite becomes more ductile and displays an enhanced resistance to temperature, compared to carbon/epoxy and glass/epoxy.

The SEM micrograph shown in Fig. 3f, confirms that KL composite presents good fiber/matrix adhesion, with little fiber slippage. The fibers are coated with matrix and the

failure occurred by both matrix cracking and fiber breakage, improved interfacial adhesion between Kevlar fiber and epoxy matrix. Whereas in the case of CL and GL, interfacial debonding and fibers pullout can be observed in Fig. 3d and e. Also, the clean fiber surfaces indicate a low interfacial bonding between the fibers and the epoxy matrix.

4.2.4. Influence of fiber configuration

The results show that UDL1 laminate has the highest storage modulus of 56.4 GPa at room temperature, followed by UDL2 about 45.7 GPa. These values are very close to those obtained in the static three-point bending tests. This could be attributed to the number of straight fibers parallel to the axis 0° between the clamps, thus ensuring a better distribution of the loads applied and a good energy transfer towards the two clamps. Furthermore, UDL3 and UDL4 composites have poor mechanical performance without fibers along the 0° orientation, lengthwise to the clamps. In the temperature above the $T_{\rm g}$, the storage moduli of UDL3 and UDL4 are 0.6 GPa equal to that of the matrix alone, much lower than that of UDL1 and UDL2 with values of 6.7 GPa and 5 GPa, respectively. Consequently, it can be inferred that the distribution of the loads applied to the laminates oriented at $\pm 45^{\circ}$ and 90° is primarily ensured by the matrix. The UDL3 laminated composite has a storage modulus slightly higher than that of UDL4 as a result of the cross-plies 45°. Even though the fibers are discontinuous, a certain quantity of energy is transferred.

By comparing the values of the temperature T_g measured from the maximum peak $\tan \delta$ (Fig. 7b), a slight decrease in the tan δ amplitude and a shift of T_{g} toward low temperatures (glass region) are observed for the different configurations of the laminates. UDL1 composite shows a decrease of 4.3 °C (90–85.7 °C) in the temperature T_g , slightly lower than that of UDL2 which drops by 4.6° C ($90-83.6^{\circ}$ C), and to UDL3 (8 °C). This difference in the $T_{\rm g}$ of the various laminates can be explained by a stiffening of the interfacial zones due to a better interaction between the fibers and matrix. In addition to this, the shear stress is directly impacted on the $T_{\rm g}$. Chua [33] reported that the loss factor of the temperature T_g of glass/polyester laminated composite decreases proportionally with the interfacial shear as well as with the transverse bending stress. In this case, the shear stress measured by static bending of UDL1 laminates is 7.11 GPa, larger than that of UDL2 and UDL3 with values of 3.28 GPa and 1.97 GPa, respectively. This, results from the number of fibers oriented at 90°, which have more freedom (slippage effect between plies and resin) on the horizontal plan and in the same direction as the shear stress. Consequently, the slippage between the layers is more significant for UDL2 and UDL3 laminates, and thus, a lower $T_{\rm g}$ compared to UDL1 laminate.

5. Conclusion

The influence of temperature, frequency, the type of reinforcements and their orientations on the mechanical and viscoelastic behavior of composite laminates has been determined by using dynamic mechanical analysis DMA in flexure. The results indicate that the storage modulus decreases with increasing the temperature for all laminates

due to increased motion of molecule strings. At $25\,^{\circ}$ C, the results of storage modulus of the laminates were found to be very close to the modulus measured in static three-point bending. The composite laminates exhibit a great stiffness (high storage modulus) when a maximum of fibers are oriented along the axis between the clamps, and the highest modulus has been reported for UDL1 composite with a value of 56.4 GPa. Thus, the glass transition temperature decreases when a maximum of fibers are oriented at $90\,^{\circ}$ due to a sliding of the layers relative to one another. The increase in frequency gave rise to a change in $T_{\rm g}$ at high temperatures for all laminates, and the maximum was measured for the KL composite ($17.6\,^{\circ}$ C), which exhibited a good interfacial interaction between fibers and matrix.

The analysis of the viscoelastic behavior of the matrix is found to be strongly affected by the presence of fibers: we are dealing here with a mechanical coupling phenomenon. It is interesting to note that the glass transition temperature of the CL and GL composites was found to be shifted to lower temperature, while an increase of 12.5 °C in the $T_{\rm g}$ of the KL laminate was observed. This is related to a better fiber/matrix interaction between epoxy matrix and Kevlar fibers. The organic nature of both components offers a better adaptation (higher deformation). Furthermore, the storage modulus of KL laminate is the lowest in the glassy region (below $T_{\rm g}$), but higher in the rubbery region compared to other laminates.

References

- [1] F. Ducept, P. Davies, D. Gamby: Compos. Part A-Appl. Sci. Manuf. 28 (1997) 719 729. DOI:10.1016/S1359-835X(97)00012-2
- [2] S.S. Pendhari, T. Kant, Y.M. Desai: Compos. Struct. 84 (2008) 114–124. DOI:10.1016/j.compstruct.2007.06.007
- [3] C.L. Schutte: Mater. Sci. Eng. R. 13 (1994) 265 323. DOI:10.1016/0927-796X(94)90002-7
- [4] B.C. Ray: J. Reinf. Plast. Compos. 25 (2006) 1227–1240. DOI:10.1177/0731684406059783
- [5] S. Sethi, B.C. Ray: Adv. Colloid Interface Sci. 217 (2015) 43 67. DOI:10.1016/j.cis.2014.12.005
- [6] L.C. Bank, T.R. Gentry, A. Barkatt: J. Reinf. Plast. Compos. 14 (1995) 559–587. DOI:10.1177/073168449501400602
- [7] V. Bellenger, J. Decelle, N. Huet: Composites Part B 36 (2005)
- 189–194. DOI:10.1016/j.compositesb.2004.04.016
 [8] P. Combette, I. Ernoult: Physique des polymères: propriétés mé-
- caniques, Presses inter Polytechnique, Canada (2005). [9] Y. Bai, T. Keller, T. Vallée: Compos. Sci. Technol. 68 (2008)
- 3099–3106. DOI:10.1016/j.compscitech.2008.07.005 [10] K. Jayaraman, K. Reifsnider: Compos. Sci. Technol. 47 (1993)
- 119–129. DOI:10.1520/CTR10391J
 [11] P. Böer, L. Holliday, T.H.K. Kang: Constr. Build. Mater. 48
- (2013) 360–370. DOI:10.1016/j.conbuildmat.2013.06.077 [12] A.S. Crasto, R.Y. Kim: J. Reinf. Plast. Compos. 12 (1993) 545–
- 558. DOI:10.117/073168449301200505
- [13] V.G. Geethamma, G. Kalaprasad, G. Groeninckx, S. Thomas: Composites Part A 36 (2005) 1499–1506. DOI:10.1016/j.compositesa.2005.03.004
- [14] W.K. Goertzen, M.R. Kessler: Composites Part B 38 (2007) 1–9. DOI:10.1016/j.compositesb.2006.06.002
- [15] L.A. Pothan, C.N. George, M.J. John, S.Z. Thomas: J. Reinf. Plast. Compos. 29 (2009) 1131–1145. DOI:10.1177/0731684409103075
- [16] K.P. Menard: Dynamic mechanical analysis: a practical introduction, CRC press (2008). DOI:10.1201/9781420053135
- [17] M.A.L. Manchado, M. Arroyo: Polymer 41 (2000) 7761–7767. DOI:10.1016/S0032-3861(00)00152-X
- [18] M.A. Sawpan, P.G. Holdsworth, P. Renshaw: Mater. Des. 42 (2012) 272–278. DOI:10.1016/j.matdes.2012.06.008
- [19] M. Akay: Compos. Sci. Technol. 47 (1993) 419–423. DOI:10.1016/0266-3538(93)90010-E

- [20] J.L. Thomason: Polym. Compos. 11 (1990) 105 13. DOI:10.1002/pc.750110206
- [21] A.A. Khatibi, Y.-W. Mai: Composites Part A 33 (2002) 1585– 1592. DOI:10.1016/S1359-835X(02)00117-3
- [22] V.M. Karbhari, Q. Wang: Composites Part B 35 (2004) 299–304. DOI:10.1016/j.compositesb.2004.01.003
- [23] D. Romanzini, A. Lavoratti, H.L. Ornaghi, S.C. Amico, A.J. Zattera: Mater. Des. 47 (2013) 9–15. DOI:10.1016/j.matdes.2012.12.029
- [24] A.N. Towo, M.P. Ansell: Compos. Sci. Technol. 68 (2008) 925–932. DOI:10.1016/j.compscitech.2007.08.022
- [25] J.D.D. Melo, D.W. Radford: Compos. Struct. 70 (2005) 240 253. DOI:10.1016/j.compstruct.2004.08.025
- [26] J.M. Berthelot: Composite materials: mechanical behavior and structural analysis, Springer, New York (1999). DOI:10.1007/978-1-4612-0527-2
- [27] ASTM D790: ASTM International, West Conshohocken, PA (2002). DOI:10.1520/D0790-02
- [28] ASTM D4065: ASTM International, West Conshohocken, PA (2001). DOI:10.1520/D4065-01.
- [29] ASTM D5023: ASTM International, West Conshohocken, PA (2001). DOI:10.1520/D5023-01
- [30] A.R. Bezazi, A. El Mahi, J.M. Berthelot, B. Bezzazi: Strength Mater. 35 (2003) 149–161. DOI:10.1023/A:1023762528362
- [31] J. Zhang, K. Chaisombat, S. He, C.H. Wang: Mater. Des. 36 (2012) 75–80. DOI:10.1016/j.matdes.2011.11.006
- [32] ASTM E 1640: ASTM International, West Conshohocken, PA (1999). DOI:10.1520/E1640-99
- [33] P.S. Chua: Polym. Compos. 8 (1987) 308–13. DOI:10.1002/pc.750080505

(Received June 4, 2015; accepted September 1, 2015)

Correspondence address

Rafik Halimi
Characterization and Instrumentation Division
Welding and NDT Research Center (CSC)
Dely Brahim Road
BP 64, Cheraga-Algiers
Algeria
Tel.: +21321342019
Fax: +21321342019
E-mail: halimir@yahoo.fr

Bibliography

Web: www.csc.dz

DOI 10.3139/146.111310 Int. J. Mater. Res. (formerly Z. Metallkd.) 106 (2015) E; page 1–10 © Carl Hanser Verlag GmbH & Co. KG ISSN 1862-5282